CHEMISTRY AND CRYSTALLOGRAPHY OF DIAGENETIC, AUTHIGENIC, AND IGNEOUS POTASSIUM FELDSPAR: IMPLICATIONS FOR SEDIMENTARY PETROLOGY IN GALE CRATER, MARS. J. P. Ott[1,2], E. B. Rampe[3], R. V. Morris[3], and A. H. Treiman[2], [1]Department of Earth and Planetary Sciences, Harvard University, 20 Oxford St., Cambridge MA 02138 (jott@college.harvard.edu). [2]Lunar and Planetary Institute, USRA, 3600 Bay Area Blvd., Houston TX. [3]NASA Johnson Space Center, Houston TX.

Introduction: The Mars Science Laboratory *Curiosity's* Chemistry and Mineralogy (CheMin) instrument [1] performed X-ray diffraction (XRD) analysis of Gale Crater drill sample Windjana and found 21 wt.% nearly pure potassium feldspar in the disordered structural state of high-sanidine [2]. The source of sanidine in Windjana is not clear – it could be detrital igneous, hydrothermal, or authigenic [2], with each possible source representing widely different implications for the sedimentary history of Gale Crater and igneous evolution of sediment sources. Here, we try to constrain the origin of the Windjana sanidine by determining unit-cell (UC) parameters and compositions of sanidines from a range of environments on Earth.

Windjana (WJ) is a basaltic sandstone of the Dillinger member within the Kimberly formation, bearing augitic pyroxene (20% by weight), magnetite (12%), iron oxide spinel (12%), and pigeonite, olivine, plagioclase, and amorphous/smectitic material (~25% total) in addition to its sanidine [2]. The Kimberly formation lies in Gale Crater's interior plains (Aeolis Palus) and includes sedimentary outcrops ranging from mudstone to conglomerate, thought to be relics of a fluvial or fluvio-deltaic depositional system [3]. This fluvial system carried debris into the crater from its northern wall, to be deposited in fluvio-lacustrine and aeolian sediments [4]. The Kimberley was the site of the first detailed investigation of Gale Crater's sediments and rocks rich in alkali elements (particularly K), making WJ the only potassic, alkali-rich rock on Mars to be analyzed in-situ for its mineralogy [2,5,6]. WJ's sanidine has UC parameters **a** = 8.578 ± 0.006 Å, **b** = 13.016 ± 0.007 Å, **c** = 7.165 ± 0.007 Å, **β** = 116.0 ± 0.07°. These parameters suggest that the WJ sanidine has some Na substituent, at $Or_{87\pm5}$, $Ab_{13\pm5}$, and is in the high structure state (i.e., complete disorder of Al and Si on tetrahedral sites) [7].

On Earth, sanidine is known to form in many environments, authigenic, hydrothermal, and igneous. Although sanidine is most familiar as a product of rapid cooling of magmas, these sanidines are usually less potassic than WJ's [8]. Unfortunately, there are no mineralogical indicators of whether Windjana was affected by authigenic or hydrothermal processes. To constrain the origins of the WJ sanidine, we are acquiring a comprehensive, precisely calibrated dataset on terrestrial alkali feldspars: cell parameters, compositions, and formation conditions.

Samples and Methods: A suite of potassium feldspar-bearing rocks was assembled from a variety of locations and formation conditions, with an emphasis on basalts for their relevance to Mars. K-spar UC parameters were refined for a number of these samples and categorized according to proposed formation mechanisms: diagenesis, hydrothermal precipitation, hydrothermal replacement, or igneous processes. Literature data were compiled for additional igneous sanidine samples [9,10].

Powder samples of grain size < 20 μm were produced for XRD analysis using a rocksaw and micronizing mill. These samples were then spiked with NIST standards 640e (Si metal) and 674b (Cr_2O_3 and ZnO) in approximately equal parts with an aggregate sample-to-standard ratio of 5:3. XRD data were obtained on a laboratory instrument (PANalytical X'Pert Pro MPD) at Johnson Space Center using: Co-Kα radiation; scans from 2-80º 2Θ; 0.02º step size; and 100 seconds per step. UC parameters and phase abundances were calculated via Rietveld refinements using JADE© software. To calculate accurate UC parameters for terrestrial K-spars, sample offsets were adjusted within the refinements to achieve NIST-standards' reported UC parameters.

Sections were cut from a number of samples and analyzed on a JEOL Electron Microprobe to further constrain their chemistry and formation conditions, using 15kV, 10nA, defocused beam to ~5μm and analyzing for Si, Al, Fe, Mg, Ca, Na, K, and Ba.

Results: The distribution of UC parameters for the full range of alkali feldspars forms a quadrilateral with corners of sanidine (K-spar with full Al-Si disorder), maximum microcline (K-spar with full Al-Si order), high albite (Na feldspar with full Al-Si disorder), and low albite (**Fig. 1, 2**). In **Fig. 1**, we compare the **b** and **c** cell lengths of Windjana's sanidine to those from our sample suite. WJ is positioned slightly down the high-sanidine, high-albite series ($Or_{87\pm5}$). **Fig. 2** gives a similar distribution, comparing the **b** and **a** cell lengths. Both distributions show a relationship between UC parameters and formation environment. This relationship can be expected since sanidine's formation conditions control its composition and the ordering of Al and Si on its tetrahedral sites. Diagenetic/authigenic feld-

spars, specifically, can be seen to exhibit less Al-Si disorder than WJ's sanidine and than is common in igneous K-spar.

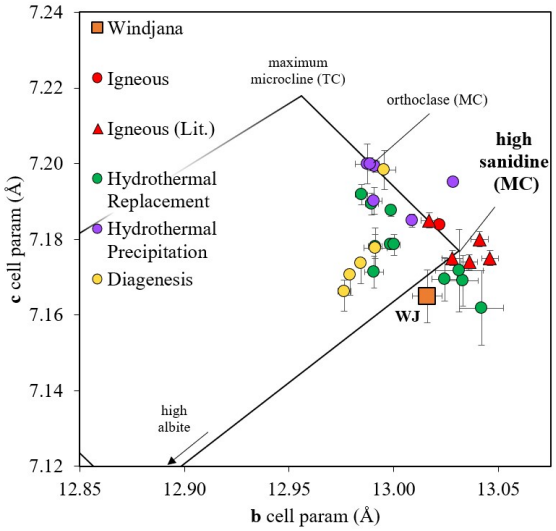

Figure 1: Sanidine **c** and **b** unit-cell dimensions, comparing terrestrial sanidines with WJ's. Low and high albite endmembers occupy the lower left and lower right corners, respectively. 1σ error bars calculated in JADE© during Rietveld refinement. Quadrilateral from [7,11-13].

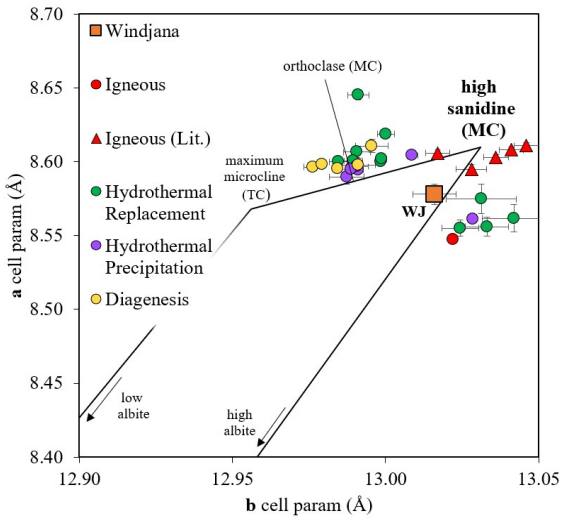

Figure 2: Sanidine **a** and **b** unit-cell dimensions [7,11-13].

Discussion: Initial interpretation of the distribution of UC parameters in **Fig. 1** suggests that the points fall into skewed quadrants, with the upper left region (relatively greater **c** length, smaller **b** length) dominated by sanidines produced by hydrothermal precipitation, the upper right region by igneous processes, the lower left by diagenesis, and the lower right by hydrothermal replacement. The hydrothermal replacement region of **Fig. 1** centers around **b** = 13.008 Å, **c** = 7.177 Å. In terms of standard deviations (σ) from regions' mean **b** and **c** lengths, Windjana plots 1.4 σ from the hydrothermal replacement mean and 3.0-6.0 σ from every other region. In **Fig. 2**, Windjana is again closest to the hydrothermal replacement region (0.70 σ), and 1.4-6.0 σ from other regions.

Conclusions: These data demonstrate that sanidine's formation environment does indeed affect its unit-cell parameters, at least to the extent that four distinct, overlapping regions can be seen in the **b** versus **c** parameter plot (**Fig. 1**), with each region corresponding to a possible formation mechanism. These regions are also present in the **b** versus **a** parameter plot, although they display greater overlap and provide less insight into Windjana's sanidine's origin as WJ plots near the boundary of overlapping regions.

The proximity of Windjana's sanidine to the hydrothermal replacement region (**Fig. 1, 2**) is consistent with formation under hydrothermal conditions, conceivably impact-induced (given the setting of Windjana in an impact crater). However, the extent of overlap between the unit-cell parameters of igneous and hydrothermal sanidine does not preclude an igneous origin. The Al-Si ordering exhibited by analyzed diagenetic/authigenic feldspars sheds doubt on those mechanisms as origins for the disordered Martian sanidine but not to the point of exclusion.

If Windjana's sanidine were igneous, it would support models of it as a fluvial and eolian reworking of igneous progenitors from Gale Crater's northern rim [2]. If the sanidine is indeed a result of hydrothermal alteration of plagioclase progenitors, then it would add to previous evidence of Martian hydrothermal processes and research on hydrothermal sanidine as a process analogue for sanidine in Gale Crater [14-16].

References: [1] Blake D. F. et al. (2012) *Space Sci. Rev., 170*(1–4), 341–399. [2] Treiman A. H., et al. (2016) *J. Geophys. Res. Planets, 121*, 75–106. [3] Le Deit L. et al. (2016) *Journal of Geophysical Research Planets*, 121(5):784-804. [4] Grotzinger J. P. et al. (2015) *Science*, *350*(6257). [5] Wray J. J. et al. (2013) *Nat. Geosci.,* 6(12), 1013–1017. [6] Carter J. and F. Poulet (2013) *Nat. Geosci., 6*(12), 1008–1012. [7] Kroll H. & Ribbe P.H. (1987) *Am. Min.* 72, 491-506. [8] Gupta A. K. (2015) 536 pp., Springer, New York, doi:10.1007/978-81-322-2083-1. [9] Scambos T. A. et al. (1987) *American Mineralogist, 72,* 973-978. [10] Ferguson R. B. et al. (1991) *The Canadian Mineralogist*, *29*, 543-552. [11] Wright T.L. & Stewart D.B. (1968). *Am. Min.* 53, 38-87. [12] Cerny P. (1986) *Can. Min*. 24, 117-128. [13] Arnaudov V. & Arnaudov R. (1997) *Geochemistry, Mineralogy, Petrology* 32, 17-21. [14] Morris R. V. et al. (2018) *LPSC49*, #2083. [15] Yen A. S. et al. (2017) *EPSL, 471*, 186-198. [16] Schwenzer S.P. et al. (2012) *Planet. Space Sci.* 70, 84-95.